SCIENCE CHINA
Earth Sciences

• RESEARCH PAPER •

June 2010 Vol.53 No.6: 911–918
doi: 10.1007/s11430-010-0051-x

# Sensitivity of sea ice and ocean simulations to sea ice salinity in a coupled global climate model

LIU JiPing*

*State Key Laboratory of Numerical Modeling for Atmospheric Sciences and Geophysical Fluid Dynamics, Institute of Atmospheric Physics, Chinese Academy of Sciences, Beijing, 100029, China*

Received February 18, 2009; accepted January 11, 2010; published online March 30, 2010

The impacts of the spatiotemporal variations of sea ice salinity on sea ice and ocean characteristics have not been studied in detail, as the existing climate models neglect or misrepresent this process. To address this issue, this paper formulated a parameterization with more realistic sea ice salinity budget, and examined the sensitivity of sea ice and ocean simulations to the ice salinity variations and associated salt flux into the ocean using a coupled global climate model. Results show that the inclusion of such a parameterization leads to an increase and thickening of sea ice in the Eurasian Arctic and within the ice pack in the Antarctic circumpolar region, and a weakening of the North Atlantic Deep Water and a strengthening of the Antarctic Bottom Water. The atmospheric responses associated with the ice changes were also discussed.

**sea ice salinity, coupled global climate model, Arctic and Antarctic**

**Citation:** Liu J P. Sensitivity of sea ice and ocean simulations to sea ice salinity in a coupled global climate model. Sci China Earth Sci, 2010, 53: 911–918, doi: 10.1007/s11430-010-0051-x

Sea ice is an important component of the climate system and an early indictor of climate change [1–3]. Sea ice acts as an insulating layer, moderating exchanges of heat, moisture, momentum, and $CO_2$ between the atmosphere and the ocean at high-latitudes. Sea ice interacts with the broader climate system through the positive ice albedo-temperature feedback, which amplifies the projected warming at high-latitudes, and through the ocean buoyancy feedback involving the growth and melt of sea ice, which influences the global thermohaline circulation (i.e., the North Atlantic Deep Water and the Antarctic Bottom Water).

The implementation of a sea ice component that accurately simulates sea ice mass balance, interfacial fluxes, and associated feedbacks with the atmosphere and the ocean into coupled global climate models (CGCMs) has received considerable attention in the global climate modeling community for the past decade. One factor motivating such improvement is the enhanced climate sensitivity at high-latitudes, particularly in the Arctic [2, 3]. Another factor is the increasing observational evidence of remarkable changes in various aspects of polar climate (i.e., the dramatic decrease of the Arctic sea ice cover and thickness [4, 5]), which requires mechanistic understanding and appropriate representation in climate simulations.

Observations suggest that the presence of salinity in sea ice has a substantial influence on the physical, thermodynamic, and mechanical properties of sea ice (i.e., associated with temperature, the ice salinity determines the brine-solid ice phase equilibrium [6]), and ocean buoyancy (i.e., associated with the growth and melt of sea ice, the salt flux influences the oceanic density stratification and deep water formation [7]).

The salinity of sea ice evolves as follows. Brine pockets are entrapped initially in sea ice during the growth process. The amount of salt entrapped increases with the salinity of

*Corresponding author (email: jliu@lasg.iap.ac.cn )

the seawater and with the growth rate of sea ice. A typical salinity value for newly-formed ice in the Arctic is ~14 psu, compared with ~30 psu for the upper Arctic Ocean [8]. As the ice continues to grow by freezing at the bottom, the amount of salt entrapped diminishes gradually as the growth rate decreases. However, the cooling of the upper part of the ice results in brine expulsion that allows the salinity in the lower part of the ice to remain high. By the time the ice thickness approaches ~40 cm, brine channels are developed and gravity drainage promotes desalination. At the onset of melting, flushing by fresh water occurs. The ice that has survived a summer melt season hence has substantially lower salinity than does the first-year ice. Thus, the ice salinity varies vertically, horizontally, and in time. However, the existing climate models neglect or misrepresent the spatiotemporal variations of the ice salinity. For example, most CGCMs assume the ice salinity to be fixed vertically and in time. Hence, the potential role of the ice salinity variations and associated salt flux into the ocean in the determination of sea ice and ocean simulations has not been studied in detail.

In an attempt to address the impacts of the spatiotemporal variations of the ice salinity on sea ice and ocean characteristics, this study developed a parameterization with more realistic ice salinity budget, and then examined the sensitivity of sea ice and ocean simulations to such a parameterization using the NASA Goddard Institute for Space Studies (GISS) CGCM.

## 1 Model description and data

Here, the author restricted detailed description to sea ice thermodynamics of the NASA GISS CGCM. Descriptions of sea ice dynamics of the NASA GISS CGCM can be found in Liu et al. [9].

The sea ice model is calculated on the same grid resolution as the atmosphere and ocean components (4° in latitude by 5° in longitude). The ice thermodynamics conserves ice mass and energy. There are four variable thickness thermal layers in the ice, and any snow amount is assumed to be in the first thermal layer. The basic sea ice growth and decay is controlled by the conduction of heat through the ice and the balance of fluxes at its upper and lower interfaces. Calculations are performed separately for the ice covered portion and the open ocean portion of the grid box. If the ice-ocean fluxes in the sea ice covered fraction extract sufficient heat from the ocean to cool the mixed layer to the freezing point, subsequent cooling causes sea ice to thicken. When surface fluxes calculated from the atmospheric model cause the mixed layer in the open ocean fraction to cool to the freezing point, sea ice forms subsequently with the minimum thickness (0.2 m) and areal concentration required to conserve energy.

The sea ice model uses the "ice bath" hypothesis (i.e., any excess energy in the first layer of the ocean model is used to melt sea ice if relevant). This effectively keeps the ocean at the freezing point in the presence of sea ice. If the horizontal open ocean fraction becomes less than a calculated lead fraction (0.06 divided by sea ice thickness), then sea ice cover is contracted horizontally to meet this calculated lead fraction and increases its thickness (conserving mass and energy). Any changes to the ice thickness imply a rearrangement of the thermal layers. The resulting heat and tracer fluxes use a simple upstream scheme. Sea ice is considered to contain no salt, and therefore as sea ice forms, brine rejection is total. Snow can be compacted into ice as a function of snow thickness, rainfall, and surface melt. Surface albedo considers both the spectral discretization in four spectral intervals and dependence on the solar zenith angle. Five surface types are included: dry snow, wet snow, bare ice, melt ponds, and open water.

To evaluate the model results, sea ice concentrations (SICs) derived from the Scanning Multichannel Microwave Radiometer and Special Sensor Microwave/Imagers for the period 1979–1999 were used [10]. The climatology of SICs was calculated and interpolated to the model grid for comparisons.

## 2 Sensitivity experiment: implementation and results

Two experiments were conducted: 1) a control experiment (hereafter referred to as CE), and 2) a sensitivity experiment, in which we included a more realistic sea ice salinity budget (hereafter referred to as SE, see detailed discussion below).

In CE of the NASA GISS CGCM, sea ice contains no salt. As sea ice grows thermodynamically, brine rejection is total. Full brine rejection increases the salinity of the uppermost ocean layer. These results in weak vertical density stratification and excessive grid-scale convection, which tends to bring relatively warm deep water to the surface and encourage sea ice melt. As discussed in the introduction, in reality, when seawater freezes, brine pockets are entrapped in the ice, while the reminder of the salt is rejected into the ocean. As the ice thickens and ages, brine drainage occurs, resulting in the older ice having lower salinity than the younger ice.

Based on observations, the author developed a parameterization that allows sea ice salinity in SE evolve as follows (conserving the salinity budget). Specifically, substantial amounts of brine from the first ocean layer (35% of the sea surface salinity) are initially entrapped in the newly-formed sea ice below the old ice or in the open ocean. Any changes to salinity within sea ice imply a rearrangement of the thickness thermal layers. Re-layering uses the (diffusive) upstream scheme for salt advection. As sea ice thickens and ages, the amount of salt entrapped in the ice exponentially decreases (rejected into the ocean) to a minimum value of

3.2 psu with a decay time of one month.

Each experiment was run for 40 years, starting from a 40-year spin-up with 1950 atmospheric composition (i.e., $CO_2$). Results are shown for the average over the last 10-year of the model simulation. For a 40-year control run, the similarity between the 3rd 10-year average and the 4th 10-year average shows that the 40-year simulations are generally sufficient to establish the first order (thermodynamic and dynamic) differences between the sensitivity and control simulations in polar regions [9].

As shown in Figure 1, the simulated SICs for both the northern and southern high-latitudes in CE (Figure 1(c), (d))

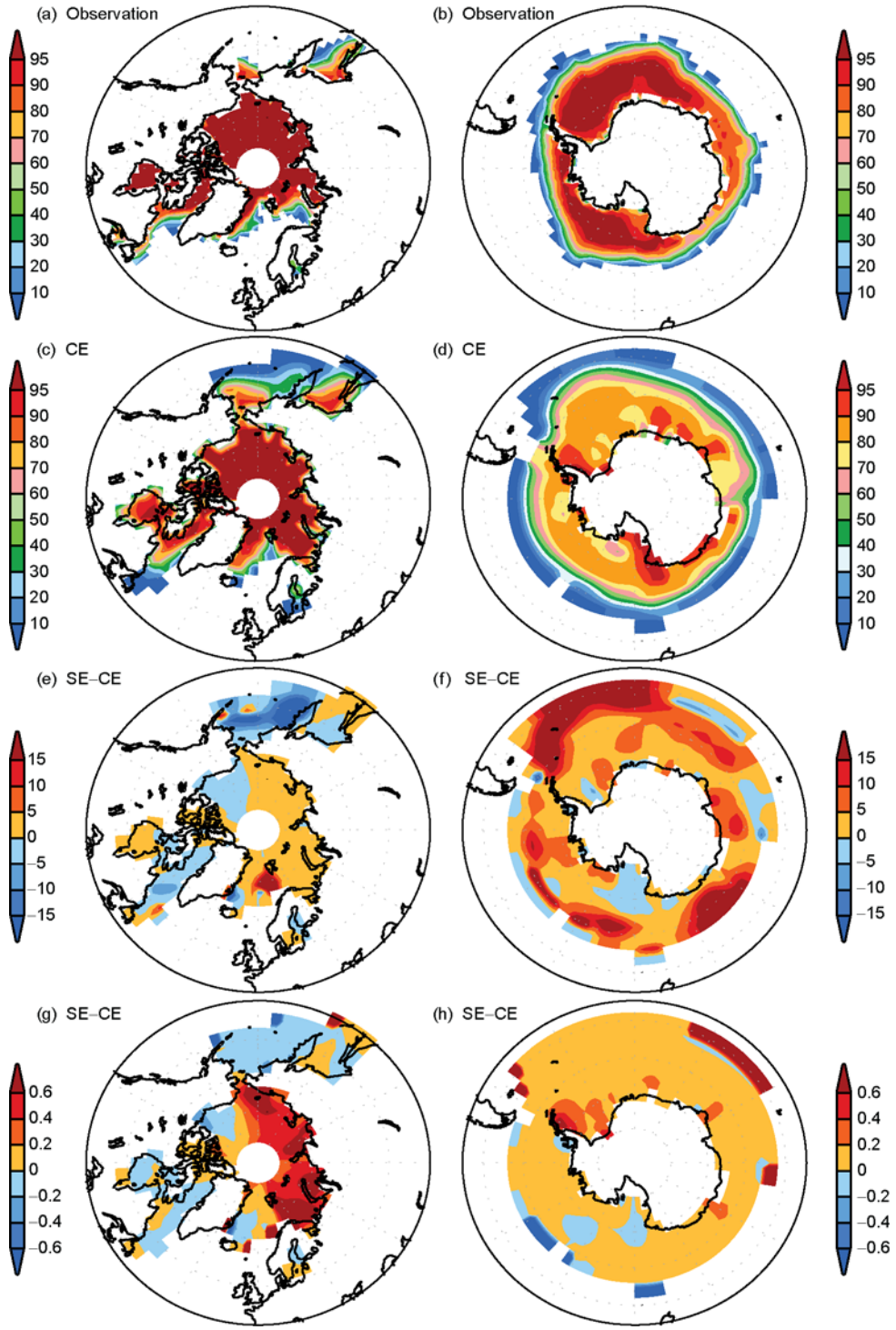


**Figure 1** Sea ice concentrations (%) in the Arctic (February, left panel) and Antarctic (September, right panel). (a) and (b) Satellite observations; (c) and (d) CE; (e) and (f) differences between SE and CE; (g) and (h) similar to (e) and (f) but for the annual mean sea ice thickness (m).

are in reasonable agreement with observations (Figure 1(a), (b)), although some regional differences are noticed (i.e., the modeled ice edges are too far south in the Bering Sea and the modeled SICs inside the pack in the Antarctic are underestimated). The simulated annual mean sea ice thickness for the entire Arctic (3.25 m) and Antarctic (0.46 m) in CE is also comparable to observations, although the model cannot well reproduce the observed thin ice in the Eurasia basin and pressure-ridged thick ice against the Canadian Archipelago and northern Greenland Sea [11]. The model captures the observed structure of the North Atlantic Deep Water (NADW, Figure 3(a)), but the modeled strength is weaker than the observations.

Figure 1(e) and (f) shows the response of SICs in the month with the maximum sea ice extent for the northern (February) and southern (September) high-latitudes to the improved representation of sea ice salinity. In the northern high-latitudes, compared to CE, SE exhibits an increase of sea ice in the Eurasian Arctic, with the pronounced increase in the central Greenland-Iceland-Norwegian (GIN) Seas, and a reduction of sea ice in the Bering Sea, Beaufort Sea, and Baffin Bay/Davis Strait. The similar spatial pattern is also found in September (the month with the minimum sea ice extent), but confined to the Arctic Ocean (not shown). In the southern high-latitudes, sea ice increases for almost the entire Antarctic in SE relative to CE. The changes in the annual mean Arctic and Antarctic sea ice thickness from CE to SE (Figure 1(g), (h)) show similar patterns to the changes in SICs in the Arctic and Antarctic from CE to SE. However, the ice thickness in the Eurasian Arctic increases dramatically (~0.4–0.6 m) in contrast to insignificant change in the Canadian Arctic.

Figure 2 shows the spatial distributions of the simulated sea ice salinity in SE. In the Arctic, high values of sea ice salinity are found at the sea ice edge zones such as the Bering Sea, the Sea of Okhotsk, and Hudson/Baffin Bay, while low values of sea ice salinity are found in the interior of the Arctic Ocean. This generally agrees with the observations since the sea ice edge zones are dominated by the first-year ice with high salinity, whereas the interior of the Arctic Ocean is dominated by the multi-year ice with low salinity. In the Antarctic, sea ice salinity generally decreases from the coastal regions and inside the ice pack to sea ice edge zones, which is somehow opposite to the spatial pattern in the Arctic, since most sea ice in the Antarctic is formed near the coastal regions (younger ice) and then advected equatorward (older ice) [12].

Figure 3(c) and (d) shows the response of the vertical temperature and salinity profile along 2.5°W in the North Atlantic sector of the Arctic to the improved representation of sea ice salinity. It appears that the upper ocean layer in SE is slightly colder relative to CE, which encourages sea ice growth. More importantly, the upper ocean layer in SE becomes fresher as compared to CE. This reduces the density contrast of the upper ocean layer, and enhances the effect of the cold halocline in the Arctic Ocean. This is consistent with the aforementioned increase of sea ice in the GIN Seas in SE relative to CE. In addition, the freshening of the upper ocean layer results in strong stratification and less connective activity in the North Atlantic. Figure 4b shows the response of the Atlantic meridional overturning circulation to the improved representation of the ice salinity. The NADW in SE, particularly between 30° and 75°N, is significantly weaker as compared to CE. The largest reduction of NADW, on the magnitude of ~2.5 Sv, is found at the depth of ~500 m at ~50°–55°N. Figure 3(g) and (h) shows the response of the vertical temperature and salinity profile along 27.5°W in the Weddell Sea. The upper ocean layer in the north Weddell Sea in SE is colder as compared to CE, which is consistent with more sea ice there (Figure 1(f)). In

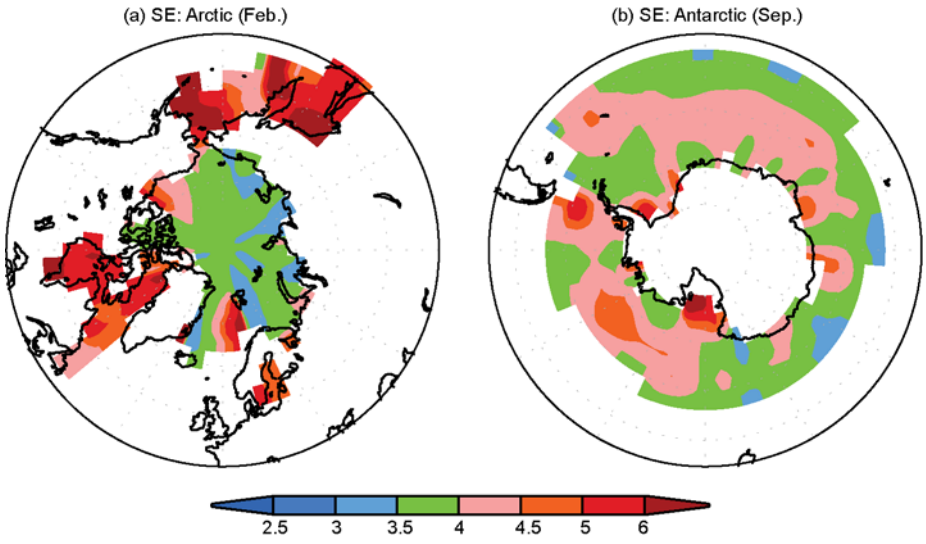


**Figure 2** Spatial distributions of sea ice salinity (psu) in SE. (a) Arctic (February), (b) Antarctic (September).

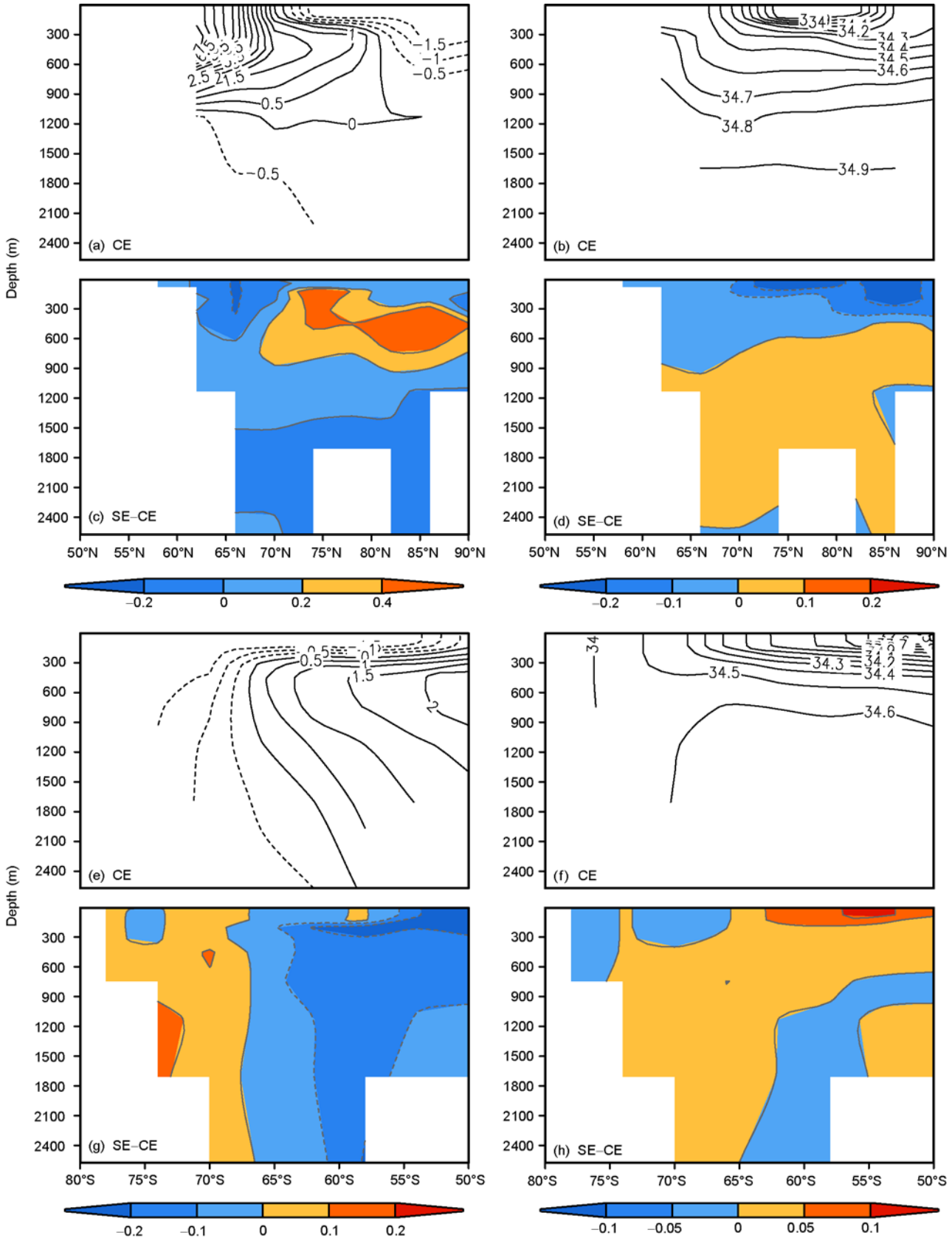


**Figure 3** Vertical ocean temperature (°C, left panel) and salinity (psu, right panel) profiles. (a)–(d) Along 2.5°W in the north Atlantic sector of the Arctic (February); (e)–(h) along 27.5°W in the Weddell Sea (September).

contrast to the decrease of ocean salinity in the North Atlantic, the salinity of the upper ocean layer in the north Weddell Sea (~60°S) increases, resulting in weak stratification. The combination of the changes in the temperature and salinity leads to an enhanced Antarctic Bottom Water (AABW) in SE as compared to CE (Figure 4(b)). Thus, the response of the NADW and AABW to the improved representation of sea ice salinity shows an out-of-phase relationship. Previous studies [13, 14] have suggested changes of freshwater inputs in key high-latitude regions can drive the bipolar seesaw between the NADW and AABW.

The evidence shows that sea ice fluctuations are meteorologically important locally, primarily through changing air-sea turbulent heat fluxes and surface albedo [15]. In the northern high-latitudes, the response of surface air temperature (SAT) shows a dipole pattern characterized by a cooling in the Kara Sea and Barents Sea (~4°–5°C) and a warming in the eastern Bering Sea and Alaska (~3–5°C), which resembles the changes of SICs (Figure 5(a)). Associated with the changes of SICs, there is an above-normal surface pressure (SP) over the central Arctic and a below-normal SP over the Bering Sea and North Atlantic (Figure 5(c)). The negative SP over the Bering Sea strengthens the Aleutian Low, which also results in anomalous advection of warm air into Alaska and the Beaufort Sea and limits sea ice growth there. In general, the changes of sea ice are in positive correlation with SP. However, the negative correlation is found in the North Atlantic, suggesting that sea ice changes are not a direct determinant of the SP changes there. Other factors including changes in temperature gradients, wave propagation etc. may be important. In the Southern high-latitudes, the enhanced sea ice cover and thickness in the Antarctic is associated with negative SAT and positive SP anomalies in almost the entire circumpolar regions (Figure 5(b), (d)). Our results also suggest that the weak pressure gradients in the circumpolar region associated with the weak polar high over the ice cap and circumpolar lows in CE are probably not related to sea ice thermodynamics. Recent investigations suggest that the poorly resolved stratospheric dynamics in the model may be important [16].

## 3 Discussion and conclusions

In this study, the author formulated a parameterization for the spatiotemporal variations of sea ice salinity, and examined its importance for sea ice and ocean simulations. The preliminary results suggest that sea ice and ocean simulations are sensitive to the improved representation of the ice

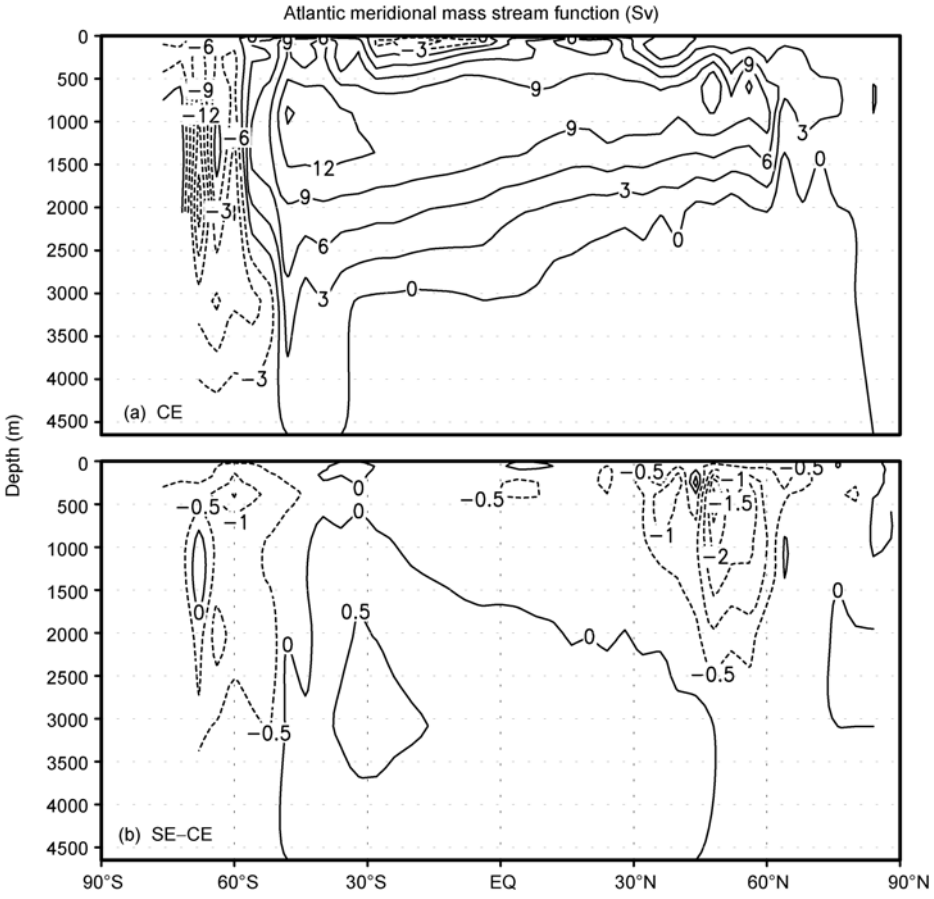


**Figure 4** The Atlantic meridional mass streamfunction (Sv). (a) CE, (b) differences between SE and CE.

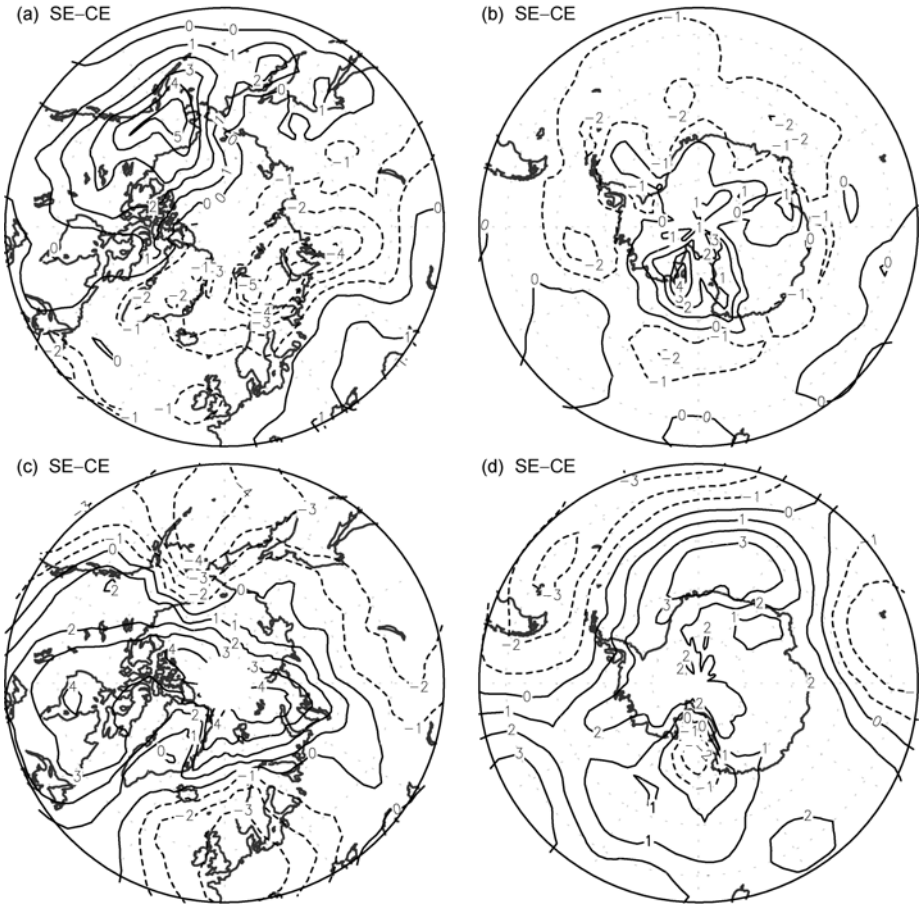


**Figure 5** Surface air temperature (°C, upper panel) and surface pressure (hPa, lower panel) differences between SE and CE. (a) and (c) Arctic (February); (b) and (d) Antarctic (September).

salinity. The inclusion of the ice salinity results in the increase and thickening of sea ice in the Eurasian Arctic, which is attributed to two processes: 1) less salt rejection into the ocean in SE freshens the upper ocean layer and weakens vertical convection as compared to CE, which encourages sea ice growth; 2) the significant weakening of NADW in SE reduces the poleward oceanic heat transport as compared to CE, which tends to cool the high-latitude north, and is helpful for generating more sea ice there. In addition, there is an increase and thickening of sea ice within the ice pack around the Antarctic and a strengthening of the AABW in the Atlantic. Although SE is an improvement as compared to CE from physical perspective, SE does not lead to much better simulations relative to CE. One of the reasons is that here we only consider the effects of including a passive sea ice salinity budget on sea ice and ocean simulations. There is also an important thermodynamic effect of the ice salinity variations related to the contraction and expansion of internal brine pockets, which increases the effective heat capacity of the ice, particularly in warm conditions. Implementing such a scheme remains a priority for future improvements of the code.

In summary, the author has shown previously [9] and here that the polar climate (i.e., sea ice) in the CGCMs is highly sensitive to both the local ice thermodynamics and dynamics, and subgrid-scale ocean processes. Unfortunately, the order of magnitude of the sensitivity is similar for both cases, and diagnosing the sources of remaining discrepancies is a complicated process. It is, however, clear that increasing the physical verisimilitude of the parameterizations is necessary.

*This research was supported by the Hundred Talents Program of the Chinese Academy of Sciences, National Basic Research Program of China (Grant No. 2006CB403605), National Natural Science Foundation of China (Grant Nos. 40876099, 40930848), High-tech R & D Program (Grant No. 2008AA121704), and China Meteorological Administration (Grant No. GYHY200806006).*

1 Barry R, Serreze M, Maslanik J, et al. The Arctic sea ice-climate system: observations and modeling. Rev Geophys, 1993, 31: 397–422
2 ACIA. Arctic Climate Impact Assessment Scientific Report. New York: Cambridge University Press, 2004. 1042
3 IPCC. Climate Change 2007: The Physical Science Basis. Contribution of Working Group I to the Fourth Assessment Report of the Intergovernmental Panel on Climate Change. Cambridge and New York: Cambridge University Press, 2007

4 Rothrock D, Yu Y, Maykut G. Thinning of the arctic sea-ice cover. Geophys Res Lett, 1999, 26: 3469–3472
5 Comiso J, Parkinson C, Gersten R, Stock L. Accelerated decline in the Arctic sea ice cover. Geophys Res Lett, 2008, 35, doi: 10.1029/2007GL031972
6 Frankenstein G, Garner R. Equations for determining the brine volume of sea ice from –0.5ºC to –22.9ºC. J Glaciol, 1967, 6: 943–944
7 McPhee M, Kottmeier C, Morison J. Ocean heat flux in the central Weddell Sea in winter. J Phys Oceanogr, 1999, 29: 1166–1179
8 Levitus S, Burgett R, Boyer T. World Ocean Atlas 1994. Vol. 3, Salinity. Washington, DC: U.S. Department of Commerce, 1994. 99
9 Liu J P, Schmidt G, Martinson D, et al. Sensitivity of sea ice to physical parameterizations in the GISS global climate model. J Geophys Res, 2003, 108: 3053, doi:10.1029/2001JC001167
10 Comiso J, Cavalieri D, Parkinson C, et al. Passive microwave algorithms for sea ice concentrations: A comparison of two techniques. Remote Sens Environ, 1997, 60: 357–384
11 Bourke R, Garrett R. Sea-ice thickness distribution in the Arctic Ocean. Cold Reg Sci Technol, 1987, 13: 259–280
12 Eicken H. Salinity profiles of Antarctic sea ice: Field data and model results. J Geophys Res, 1992, 97: 15545–15557
13 Broecker W. Paleocean circulation during the last deglaciation: A bipolar seesaw? Paleoceanography, 1998, 13: 119–121
14 Weaver A, Saenko O, Clark P, et al. Meltwater pulse 1A from Antarctica as a trigger of the Bolling-Allerod warm interval. Science, 2003, 299: 1709–1713
15 Walsh J. The role of sea ice in climate variability: Theories and evidence. Atmosphere-Ocean, 1983, 21: 229–242
16 Thompson D, Baldwin M, Solomon S. Stratopshere-troposhere coupling in the Southern Hemisphere. J Atmos Sci, 2005, 62: 708–715